Real-Time NMPC for Semi-Automated Highway Driving of Long Heavy Vehicle Combinations ⋆

Niels van Duijkeren * **Tamas Keviczky** ** **Peter Nilsson** *** **Leo Laine** ***

* *KU Leuven, B-3001 Heverlee, Belgium (e-mail: Niels.vanDuijkeren@kuleuven.be).*
** *Delft University of Technology, 2628 CD Delft, The Netherlands (e-mail: T.Keviczky@tudelft.nl)*
*** *Volvo Group Trucks Technology, SE-405 08 Göteborg, Sweden (e-mail: {Peter.q.Nilsson, Leo.Laine}@volvo.com)*

Abstract: This work presents a Nonlinear Model Predictive Control (NMPC) approach to real-time trajectory generation for highway driving with long truck combinations. In order to consider all relevant information for the road and the surrounding traffic, we formulate a finite-horizon optimal control problem (OCP) that incorporates a prediction model in spatial coordinates for the vehicle and the surrounding traffic. This allows road properties (such as curvature) to appear as known variables in the prediction horizon. The objective function of the resulting constrained nonlinear least-squares problem provides a trade-off between tracking performance, driver comfort, and keeping a comfortable distance from fellow road users. The OCP is solved with a direct multiple shooting solution method implemented in a real-time iteration scheme using ACADO code generation and compared with a feedback scheme that solves the entire nonlinear program in each time step with the interior point solver IPOPT. To illustrate the efficacy and the real-time implementability of the methodology, simulation results are presented for a high way merging scenario of a long heavy vehicle combination.

Keywords: predictive control, model-based control, automotive control, autonomous vehicles, real-time MPC, control engineering, nonlinear control

1. INTRODUCTION

The so-called long heavy vehicle combinations (LHVCs) are trucks that are widely used in Canada and Australia today, and will be more abundant on the road also in Europe in the near future (Kindt et al. (2011)). They have the potential to decrease road transport costs, traffic congestions, and generate lower emissions than current means of road freight transport. However, an undesired effect of the added towed units is the increase in difficulty to maneuver these trucks on roads and in busy traffic. The increased complexity for truck drivers to handle tasks such as changing lane and maneuvering in tight corners, call for automatic driver assistance functions. Development of such advanced driver assistance systems, or potentially autonomously functioning trucks, are essential to safeguard traffic safety with an increasing use of LHVCs. One crucial element to increase autonomy in completing the complex driving task of LHVCs is the online trajectory generation algorithm. The main challenge for this trajectory generator is to combine the information about the state of the truck, the road properties, and the behavior of the surrounding traffic, and decide on a desired steering and velocity profile.

Fig. 1. LHVC in the A-double configuration.

We propose to use predictive control techniques as the trajectory generator for the following reasons. First and foremost, such techniques can plan safe vehicle maneuvers ahead to avoid need for conservatism. Secondly, by means of optimization, incorporating models for the truck, the road and surrounding traffic, the most preferential path can be selected from the set of safe trajectories. We highlight three types of control techniques that can fulfill the need for a predictive strategy with real-time performance. Nonlinear model predictive control (NMPC), randomized sampling-based planning strategies (LaValle (1998); Karaman and Frazzoli (2011)) and state-lattice

⋆ The research leading to these results was partly funded by the People Programme (Marie Curie Actions) of the European Union's Seventh Framework Programme FP7/2007-2013/ under REA grant agreement n° 607957. This work also benefits from Center-of-Excellence Optimization in Engineering (OPTEC), the Belgian Programme on Interuniversity Attraction Poles, initiated by the Belgian Federal Science Policy Office (DYSCO). The applied research on commercial heavy vehicles was funded by Volvo Group Trucks Technology (VGTT) and Virtual Prototyping Centre (ViP).

approaches combined with motion primitives (see e.g., Pivtoraiko et al. (2009)).

This paper presents an NMPC technique for longitudinal and lateral motion control of the A-double combination during highway driving in presence of surrounding vehicles. The A-double combination LHVC, depicted in Fig. 1, is currently the longest LHVC that is allowed on roads in Europe in the very near future. First, an optimal control problem (OCP) is formulated that reflects the desired motion of the truck over a finite future horizon. The prediction model considers the nonlinear articulated truck dynamics, the geometry of the road, and the behavior of the surrounding traffic. The OCP is transcribed as a Nonlinear Program (NLP) using a multiple shooting prediction model integration technique. In order to achieve real-time computations when solving this complex NLP online, the real-time iteration (RTI) scheme is employed (Diehl et al. (2005)). Since the real-time iteration scheme is a suboptimal solution technique, for comparison purposes, an interior-point NLP optimizer (IPOPT) is used to solve the NLP as well. Closed-loop simulation results are presented to show that the trajectory generator can handle complex situations while achieving real-time performance, thus enabling predictive advanced driver assistance functions to be implemented. The presented solution technique has been successfully implemented on a motion simulator platform operated by professional truck drivers at the Swedish National Road and Transport Research Institute (VTI) in Gothenburg, Sweden.

2. FORMULATION OF OPTIMAL CONTROL PROBLEM

When studying highway maneuvers of the A-double combination, additional factors need to be taken into consideration compared to regular passenger cars. One important aspect is to prevent the truck or one of its trailers to roll over due to excessive acceleration levels. Other aspects include the difficulty of keeping all trailers inside the lane boundaries and the limited agility due to the size and weight of the truck. In this section, we mathematically formulate comfortable driving behavior and incorporate the limits on agility and safety effectively as the objective and the constraints of the OCP, respectively. Additionally we present an approach to include surrounding traffic in the OCP employing a prediction of their motion.

2.1 Prediction Model

In vehicle dynamics research and engineering a wide variety of vehicle models are used. These range from non-slip kinematic car models, neglecting tire properties, to multi-body dynamical systems accurately modeling the effects of chassis dynamics and dynamic nonlinear tire models. Choosing the most appropriate model for prediction purposes naturally highly depends on the expected situations that need to be predicted. From experience we know that for mild high-speed driving maneuvers the so-called single track model for the lateral dynamics, often referred to as a bicycle model, with a linear tire slip balances complexity and accuracy very well. The most important properties of the single-track model, schematically depicted in Fig. 2, are:

- The vehicle model is planar, effects such as roll and pitch are not modeled.
- The wheels of the vehicle are lumped in the center of each axle.
- Each unit is a rigid body mass without suspension, chassis, and cabin dynamics.
- The lateral tire stiffness is assumed to be linear in the lateral tire slip.
- Coupling between longitudinal and lateral dynamics is neglected.

The lateral vehicle model and parameters used for this work, considering a fully loaded A-double combination, are reported in Nilsson and Tagesson (2013). For a more comprehensive overview of different types of vehicle models and their properties see e.g., Rajamani (2012).

In addition to the lateral vehicle dynamics of the A-double combination, the prediction model also models the longitudinal dynamics, the position on the road, and the behavior of fellow road users. Vehicle dynamics are often expressed in the non-inertial reference frame fixed in the center of gravity of a car. In order to avoid ambiguity in which frame certain measurements are defined, we denote a measurement a in point v with respect to reference frame o expressed in reference frame f by ${}^{v}_{o}a^{f}$. The subscript is reserved to refer to a specific component of the variable a and to distinguish between actual measurements and e.g., reference signals. Throughout the paper, the identifier *ref* (for reference) denotes a reference signal for the NMPC controller and the identifier *des* (for desired) denotes a reference signal for the low-level control algorithms such as the cruise controller. See Fig. 2 for a schematic representation of the single-track model for the A-double combination and important points and reference frames on the truck. The four units the A-double combination consists of: the tractor, the first semi-trailer, the converter dolly and the second semi-trailer are named unit A, B, C and D respectively.

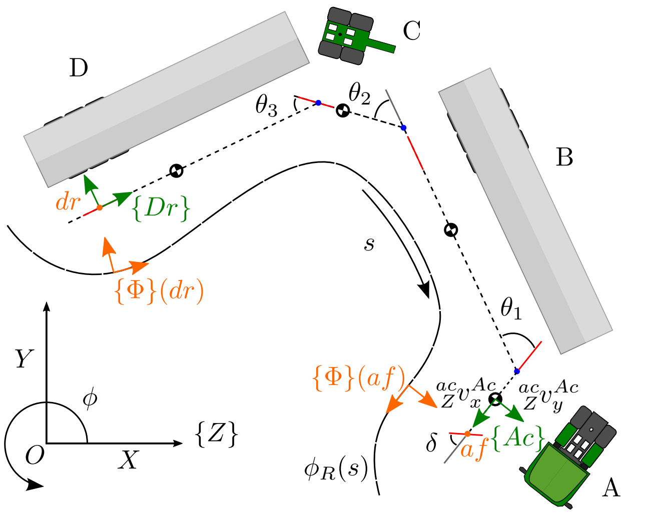

Fig. 2. Schematic representation of the single-track model of the A-double combination and an illustration for a selection of reference frames. The road curvature is exaggerated for clarity of the illustration.

The state vector ξ of the prediction model can be divided into four groups for illustrative purposes. States describing the lateral dynamics of the truck

$$\xi_{\text{lat}} = \left({}^{ac}_{Z}v_y^{Ac} \;\; \phi \;\; \dot{\phi} \;\; \theta_1 \;\; \dot{\theta}_1 \;\; \theta_2 \;\; \dot{\theta}_2 \;\; \theta_3 \;\; \dot{\theta}_3 \;\; \delta \right)^T \tag{1}$$

are governed, as previously introduced, by a single track vehicle model. The longitudinal part of the dynamics

$$\xi_{\text{long}} = \left({}^{ac}_{Z}v_x^{Ac} \;\; {}^{ac}_{Z}a_x^{Ac} \;\; {}^{ac}_{Z}a_{x,\text{des}}^{Ac} \right)^T \tag{2}$$

essentially models the closed-loop cruise-controlled system as a first-order system on the desired longitudinal acceleration with a time constant of $0.25s$. Another group of states modeling the distance of the front axle of the tractor (point af) and the rear-most axle of the second semi-trailer (point dr) from the lane center is described as

$$\xi_{\text{road}} = \left({}^{af}_{\Phi}s^{\Phi} \;\; {}^{af}_{\Phi}d^{\Phi} \;\; {}^{dr}_{\Phi}s^{\Phi} \;\; {}^{dr}_{\Phi}d^{\Phi} \right)^T. \tag{3}$$

Finally, the states that model the position of the truck with respect to surrounding traffic are denoted by

$$\xi_{\text{traffic}} = \left(\Delta s_{o,1} \;\; \Delta s_{o,2} \;\; \Delta s_{o,3} \right)^T. \tag{4}$$

In this work, the traffic model assumes that all vehicles remain driving at the measured velocity along the lane center.

The control inputs to this system are the steering angle rate for the front wheels of the tractor, and the desired longitudinal jerk (i.e., the change in acceleration) requested from the cruise-controller.

2.2 Spatial Reformulation of Prediction Model

In order to model the position of the vehicle in the curvilinear coordinate system of the road, we require knowledge on the relative heading and the curvature of the road in our prediction horizon. It is common to choose a certain time span of interest for the prediction horizon. In case of our trajectory generator, we would then need to know the road heading and curvature as a function of the vehicle states. As suggested in previous work by Gao et al. (2012); Frasch et al. (2013), a more natural choice is to take the traveled distance of the vehicle along the road geometry as a pseudo-time variable in a spatial horizon. The main advantage is that the road geometry can then be algebraically defined in the prediction horizon. The price to pay is a nonlinear transformation of the prediction model equations and the loss of the ability to explicitly define the position of fellow road users in the prediction horizon. Suppose that ${}^{af}_{\Phi}s^{\Phi}$ represents the position of the front axle of the tractor along the road geometry, then the time transformation will have the form ${}^{d\xi}/_{ds} = {}^{d\xi}/_{dt} \cdot {}^{dt}/_{ds}$. The transformation consists of dividing the system of first-order differential equations by

$$\frac{d\,{}^{af}_{\Phi}s^{\Phi}}{dt} = \frac{{}^{af}_{Z}v_x^{Af}\cos(\phi - \phi_R) - {}^{af}_{Z}v_y^{Af}\sin(\phi - \phi_R)}{1 - \kappa_R\,{}^{af}_{\Phi}d^{\Phi}} \tag{5}$$

with $\kappa_R = {}^{d\phi_R}/_{ds}$ as the local curvature of the road at ${}^{af}_{\Phi}s^{\Phi}$. An explicit overview of the prediction model equations and a more extensive treatment of its spatial reformulation is reported in Van Duijkeren (2014).

It is important to note that the heading and curvature of the road in the prediction horizon remains fixed only for one point of the vehicle. The heading and the curvature of the road at e.g., the position ${}^{dr}_{\Phi}s^{\Phi}$ of the rear trailer is not algebraically defined. This matter is dealt with by a crucial assumption: the distance between any two points of the truck along the road geometry is assumed to be constant. Considering the highway driving task, this assumption is not problematic but it makes our implementation incompatible with high curvature conditions, such as city driving. With this assumption, it also opens the possibility to describe the position ${}^{dr}_{\Phi}d^{\Phi}$ in terms of the position of the tractor and the articulation angles of the truck. However, in this work, the position ${}^{dr}_{\Phi}d^{\Phi}$ is kept as a state so that lane departure constraints can be formulated as state box constraints. With the prediction model introduced, we describe the remaining elements of the OCP formulation next.

2.3 Cost Function & Constraints

For our trajectory generator we observe that we require three distinct (possibly conflicting) objectives. The first is a tracking objective, the second part promotes smooth and comfortable trajectories, and the last part penalizes driving close to other vehicles. On the one hand, an economic-MPC (EMPC) can be formulated to optimize a generic cost function. Although this may be attractive conceptually, finding efficient solution strategies to the resulting NLPs is nontrivial. On the other hand, efficient algorithms are available for constrained least-squares optimization problems, such as the generalized Gauss-Newton algorithm. The latter type of solution strategy is especially well-suited for tracking-MPC applications because of its least-squares nature. Since real-time performance is of crucial importance, we formulate our economic objective as a least-squares optimization problem.

Tracking Objective In (12) the tracking objective is represented by three terms in the Lagrange-term of the cost function:

$$\begin{aligned} &K_{d_1}\left({}^{af}_{\Phi}d^{\Phi} - {}^{af}_{\Phi}d^{\Phi}_{\text{ref}}\right)^2 + K_{d_4}\left({}^{dr}_{\Phi}d^{\Phi} - {}^{dr}_{\Phi}d^{\Phi}_{\text{ref}}\right)^2 + \\ &\quad K_{v_x}\left({}^{ac}_{Z}v_x^{Ac} - {}^{ac}_{Z}v_{x,\text{ref}}^{Ac}\right)^2 \end{aligned} \tag{6}$$

Firstly, the lateral distance offset from the lane center for points af and dr are penalized. Secondly, to achieve efficient driving behavior (i.e., fast transportation) it is desired to drive close to the legal speed limit. A weighted quadratic penalty is placed on the tracking error of both states.

Driver Comfort Objective Previous research, such as Nilsson et al. (2014), supports the generally accepted observation that the human perception of smooth and comfortable driving is closely related to the jerk levels that arise over a driven trajectory. Hence an important part of the cost function promotes driver comfort by rewarding driving at low jerk levels. Additionally, the longitudinal acceleration levels and rapid steering are penalized resulting in the Lagrange term:

$$K_{j_x}\left({}^{ac}_{Z}j_{x,\text{des}}^{Ac}\right)^2 + K_{j_y}\left({}^{ac}_{Z}j_y^{Ac}\right)^2 + K_{a_x}\left({}^{ac}_{Z}a_{x,\text{des}}^{Ac}\right)^2 + K_{\dot{\delta}}\dot{\delta}^2 \tag{7}$$

The desired longitudinal jerk is a control input to the vehicle prediction model. The lateral jerk however is neither a state nor an input, thus we must find a closed-form expression as a function of the states and inputs. The following expression can be derived for this relationship

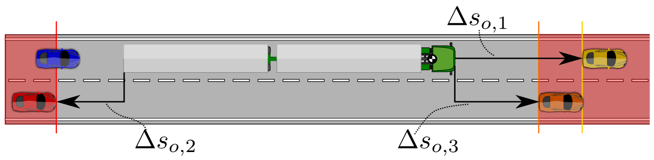

Fig. 3. Distance keeping scenario in a lane change to the right and labeling of fellow road users.

$$\begin{aligned} {}^{ac}_{Z}j_y^{Ac} = 2\,{}^{ac}_{Z}\dot{\phi}^{Z} \cdot {}^{ac}_{Z}\dot{v}_x^{Ac} + {}^{ac}_{Z}\ddot{\phi}^{Z} \cdot {}^{ac}_{Z}v_x^{Ac} + \\ - \left({}^{ac}_{Z}\dot{\phi}^{Z}\right)^2 \cdot {}^{ac}_{Z}v_y^{Ac} + {}^{ac}_{Z}\ddot{v}_y^{Ac} \end{aligned} \tag{8}$$

We note that the only unknown term is ${}^{ac}_{Z}\ddot{v}_y^{Ac}$. Fortunately, in highway driving scenarios that same term is not the greatest contributor to the lateral jerk. Since we solely need to capture the trend for the jerk level in order to penalize it, we choose to approximate the jerk with the remaining known terms.

Distance Keeping Objective Keeping distance to other traffic is a tasks that involves heuristics. For instance, one is usually insensitive to the behavior of a car far away. In a normal lane keeping scenario, only a vehicle in the near vicinity and in the same lane is of our interest. In fact by assuming that the trailing vehicle in the same lane adjusts its speed to the truck, only the vehicle in front of us needs to be taken into account. The situation becomes slightly more complex for a lane change, since two extra vehicles must be considered: the nearest preceding vehicle and the nearest trailing vehicle in the target lane. Fig. 3 illustrates this concept for a lane change scenario. The main part of the lane-changing logic behavior is captured in a preprocessing stage to the OCP solver, and sensitivity to the $\Delta s_{o,1}$, $\Delta s_{o,2}$, $\Delta s_{o,3}$ parameters is determined beforehand according to the scenario. In case a lane change is not desired or infeasible, $\Delta s_{o,2}$ and $\Delta s_{o,3}$ are not of interest to the trajectory generator and thus removed from the optimization.

The logic in the sensitivity of the distance to other vehicles is captured in the optimization problem. We choose a quadratic penalty in the Lagrange term of the OCP:

$$\sum_{k=1}^{3} K_{\Delta s_{o,k}} \left(f_{\mathrm{dk}}(\Delta s_{o,k},\, {}^{ac}_{Z}v_x^{Ac})\right)^2 \tag{9}$$

where the function f_{dk}, assuming ${}^{af}_{\Phi}\dot{s}_x^{\Phi} \approx {}^{ac}_{Z}v_x^{Ac}$, approximates

$$f_{\mathrm{dk}} = \begin{cases} 0, & \text{if } \Delta s_{o,k} > \tau_{o,k}\,{}^{ac}_{Z}v_x^{Ac} \\ \dfrac{\tau_{o,k}\,{}^{ac}_{Z}v_x^{Ac} - \Delta s_{o,k}}{\tau_{o,k}\,{}^{ac}_{Z}v_x^{Ac}}, & \text{otherwise} \end{cases} \tag{10}$$

with $\tau_{o,k}$ denoting the temporal gap at which the respective vehicle k is taken under consideration. Two alternative methods have been explored to implement this logic behavior. One is to introduce a slack variable that becomes active when crossing a distance threshold, similarly to the technique described in Borrelli et al. (2004). The second method is to use a sigmoid function to closely resemble binary behavior. We experienced no obvious differences in the resulting open-loop optimal trajectories and the closed loop behavior. In our implementation, the latter technique using a sigmoid function, resulted in significantly shorter solution times and was therefore preferred. The employed sigmoid function is

$$f_{\mathrm{dk}}(\Delta s_{o,k},\, {}^{ac}_{Z}v_x^{Ac}) = \frac{\tau_{o,k}\,{}^{ac}_{Z}v_x^{Ac} - \Delta s_{o,k}}{\tau_{o,k}\,{}^{ac}_{Z}v_x^{Ac}\left(1 + e^{-c_{o,k}\left(\tau_{o,k} - \Delta s_{o,k}/{}^{ac}_{Z}v_x^{Ac}\right)}\right)} \tag{11}$$

with $c_{o,k}$ a tuning variable for the slope of the sigmoid function in the transition region.

Complete Optimal Control Problem With the three different elements in the objective function introduced, we define our OCP.

$$\min_{\xi(\cdot),u(\cdot)} \int_{s=0}^{s_f} (6) + (7) + (9)\, d\sigma \tag{12}$$

subject to

$$\begin{aligned}
\frac{d\xi}{ds} &= f(s,\xi,u) && && \text{(13)}\\
\underline{a}_y &\le {}^{af}_{Z}a_y^{Af}(s) &&\le \overline{a}_y && \text{(14)}\\
\underline{a}_y &\le {}^{dr}_{Z}a_y^{Dr}(s) &&\le \overline{a}_y && \text{(15)}\\
\underline{d} &\le {}^{af}_{\Phi}d^{\Phi}(s) &&\le \overline{d} && \text{(16)}\\
\underline{d} &\le {}^{dr}_{\Phi}d^{\Phi}(s) &&\le \overline{d} && \text{(17)}\\
\underline{a}_{x,\mathrm{des}} &\le {}^{ac}_{Z}a_{x,\mathrm{des}}^{Ac}(s) &&\le \overline{a}_{x,\mathrm{des}} && \text{(18)}\\
\underline{\delta} &\le \delta(s) &&\le \overline{\delta} && \text{(19)}\\
\underline{\dot{\delta}} &\le \dot{\delta}(s) &&\le \overline{\dot{\delta}} && \text{(20)}\\
\underline{\Delta s}_{0,k} &\le \Delta s_{0,k} && k = 1,\ldots,3 && \text{(21)}\\
& && \forall s \in [0, s_f] &&
\end{aligned}$$

The equations of motion (13) depend on the position of the front axle of the tractor ${}^{af}_{\Phi}s$ along the road geometry, the state, and the control input. Constraints (14) and (15) limit the lateral accelerations of two points of the truck to prevent the truck to tip over. Constraints (16) and (17) enforce two points of the truck to stay inside the lane boundaries. Constraint (18) informs the trajectory generator of the physical maximum longitudinal acceleration of the truck that may depend on the position on the road (slope of road). Constraints (19) and (20) reflect the maximum road wheel angle and its time derivative, respectively, reflecting physical actuation constraints. Finally, (21) prohibits a trajectory that collides with that of one of the surrounding vehicles.

3. IMPLEMENTED SOLUTION TECHNIQUES

The OCP problem introduced in Section 2 is transcribed into an nonlinear program (NLP). The spatial prediction horizon in ${}^{af}_{\Phi}s^{\Phi}$ is discretized using 50 intervals with a step size of Δs of 2 meters. The system dynamics constraints are enforced with a multiple-shooting integration scheme using a fourth order explicit Runge-Kutta update rule taking 5 intermediate integration steps in each discretization interval of the OCP. The control inputs $\dot{\delta}$ and ${}^{af}_{Z}j_{x,\mathrm{des}}^{Af}$ are held constant over each interval. The objective function is approximated by the sum of the Lagrange terms at each shooting node of the transcribed OCP. Likewise, constraint satisfaction is enforced at each shooting node. In a lane change the reference transitions to the other lane with a minimum jerk path for a point-mass. The reference for $v_{x,\mathrm{meas}} = {}^{ac}_{Z}v_x^{Ac}$ is pre-processed to prevent a high velocity set-point in curves and to adapt the velocity to leading vehicles close-by. To attain real-time performance, the main challenge is to find a trade-off between a long prediction horizon and a fast control rate. In this work, the horizon length and the control frequency are $100m$ and $2m^{-1}$ respectively. The physical control frequency is synchronized with the NMPC control intervals of the transcribed OCP and is triggered every 2 meters traveled along the lane center. Driving at $20^{m}/_{s}$ this agrees to a control rate of $10Hz$.

Two different techniques are implemented to solve the NLP. Both solution schemes share the same base of heuristics and are entirely written in the C/C++ programming language.

(1) The so-called real-time iteration (RTI) scheme is implemented using the open-source ACADO toolkit (Houska et al. (2011)). Using the code generation functionality of ACADO, tailored C-code is generated for the SQP-type solution scheme. Both the structure of the RTI scheme, explained in e.g., Diehl et al. (2002, 2005) and the auto-generated code for the NLP solver enable very fast execution times for the NMPC solution steps. Previous results already showed solution time scales for NMPC that are well within the region that allows their application to fast mechatronic systems, see e.g., Vukov et al. (2012); Frasch et al. (2013); Verschueren et al. (2014). The active-set QP solver qpOASES is used to solve each intermediate condensed QP (Ferreau et al. (2014)).

(2) Solving the NLP to a certain prescribed accuracy with the state-of-art interior point NLP solver IPOPT, see Wächter and Biegler (2006). The NLP is formulated in the symbolic framework for algorithmic differentiation (AD) and numerical optimization CasADi, see e.g., Andersson (2013). The toolkit implements efficient techniques for AD to supply IPOPT with the gradient of the objective, the Jacobian of the constraints and the Hessian of the Lagrangian.

We note that the NLP was identical in both cases, and that the first method using the RTI scheme was fast enough for real-time application. The second implementation with IPOPT is used to compare the closed-loop performance of a suboptimal and an optimal solution technique. The next section presents the numerical results of closed-loop simulation experiments on a high-fidelity model of the A-double LHVC in a realistic highway driving scenario.

4. SIMULATION EXPERIMENTS

In order to evaluate and illustrate the results in this work, we simulate the controlled A-double combination situated in a highway scenario. A high-fidelity two-track model library developed by Volvo Trucks is used simulate the “real” truck plant model dynamics. The model includes detailed sub-models of the vehicle chassis, cab suspensions, steering system, power train, and brakes. The frame torsion flexibility of the tractor and semi-trailers is considered by using multiple frame bodies connected through springs. The Magic Formula tire model, Pacejka (2006), with combined slip, dynamic relaxation, and rolling resistance, is used for all tires in the vehicle combination. In this framework, control allocation has been used for

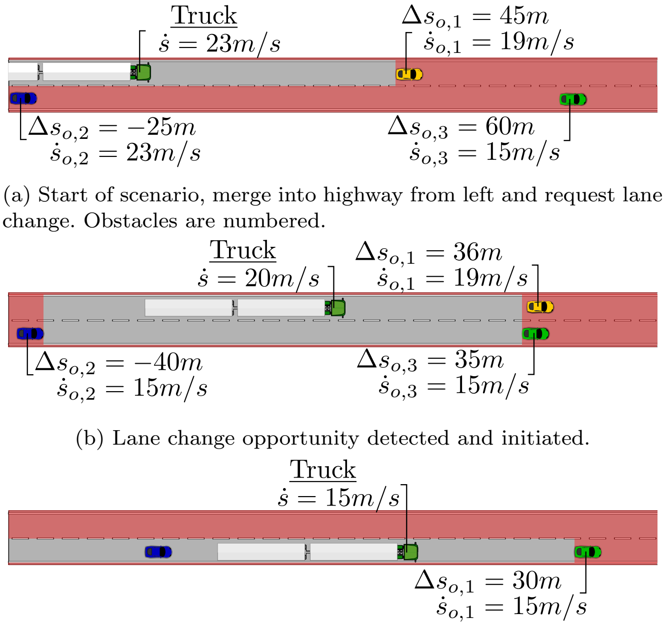

(a) Start of scenario, merge into highway from left and request lane change. Obstacles are numbered.

(b) Lane change opportunity detected and initiated.

(c) Lane change is completed. Obstacles are renumbered.

Fig. 4. Main phases of the lane change scenario.

coordinating propulsion, braking and steering as described in Laine (2007). The control allocation weighting for, e.g. braking in-between axles, has been adapted to commercial heavy vehicles (see Tagesson et al. (2009)). This simulation model is much more accurate than the prediction model used in the NMPC formulation and serves as a benchmark for the performance assessment of the NMPC applied to a realistic system.

The simulation experiments are executed in Simulink. The control algorithms, written in C/C++, are interfaced through a MATLAB s-function. We consider full-state feedback control, i.e., the required knowledge of the vehicle, the road and surrounding traffic is assumed to be available. In the simulations the truck drives autonomously and the presence of a driver in the loop is neglected.

The considered scenario is based on actual real-life concerns that arise with the introduction of the longer truck combinations. The scenario begins with the truck being in the left lane of a highway in busy traffic. The controlled vehicle can arrive there e.g., when two highways merge. The truck needs to transition to a lane to the right in order to take the next exit, but the size of the truck makes it difficult to keep an overview of the situation. We consider that a vehicle in the lane to the right is blocking the way driving with the same speed as the truck. Another obstacle in front of that vehicle drives significantly slower. Out of courtesy, the vehicle to the right slows down early to make space for the truck. In the truck its own lane, a vehicle in front drives slightly slower thus the truck speed needs to be adjusted while looking for a lane-change opportunity. In order to move to the right lane, the controller must recognize that the vehicle in the right lane keeps a gap. As soon as the gap complies with the minimum requirements, the truck needs to slow down to match the velocity of the vehicles in the adjacent lane. Finally, it can transition to the new lane and complete the merging maneuver. In

Fig. 4 three main phases of this scenario are depicted with distance and velocity observations.

Fig. 5 presents several relevant signals from the closed-loop simulation results in the introduced scenario. The employed controller parameters are outlined in Section A. We note that the legend entries d_1, d_4 and v_x refer to ${}^{af}_{\Phi}d^{\Phi}$, ${}^{dr}_{\Phi}d^{\Phi}$ and ${}^{ac}_{Z}v_x^{Ac}$, respectively. The reference signals (ref) to the NMPC controller are shown with virtual measurements (meas) originating from the high-fidelity model of the A-double combination. From Fig. 5b we can observe that before the lane change the truck slows down slightly to adapt to the velocity of the leading car. In Fig. 5d we can observe that the main trade-off is between tracking and comfortable driving. At around 21 seconds a lane change opportunity is detected and immediately the truck slows down to find the optimal distance to the obstacles in the adjacent lane. The distance to surrounding vehicles is the main contributor to the cost function of the NLP. Fig. 5a illustrates the lane transition that a few seconds later smoothly brings the truck to the right lane. When the lane change is completed, the truck slows down to track the velocity reference and to increase the gap with the new leading vehicle.

Recall that the RTI scheme, implemented by ACADO, is a suboptimal solution method. Since only one Newton step is taken for an SQP in each control interval, we do not necessarily achieve a local minimum of the NLP at all times. Additionally, the Gauss-Newton Hessian approximation employed for intermediate QPs is in general not ideal for economic type cost functions such as our distance keeping objective. In order to illustrate the effect of such a suboptimal strategy on the closed-loop performance, we show a comparison with the total objective value of NLP during the same scenario in Fig. 6a. In addition, the solution times per control iteration are provided in Fig. 6b. From the evolution of the total cost we can clearly observe a very similar trend between the RTI scheme and IPOPT. The difference between the two varies on the same order of magnitude as the objective value. The state trajectories of the system, not shown in this paper, are nearly identical as well. At the same time we can see that the RTI scheme shows solution times that are by a factor of 90 faster than IPOPT. This illustrates well the main philosophy of suboptimal methods for NMPC: it is not always necessary to have the optimal control input available. Instead, it is important to achieve real-time performance and to converge to a local optimum with a high rate that allows intermediate SQP solutions to be applied. Notice from Fig. 6b that our bound on the computational time is not constant, since it depends on the spatial control update frequency (i.e., the speed of the truck).

The scenario described above considered a straight road. We chose to present the results of this scenario for ease of interpretation. The implemented control algorithms however are entirely compatible with curved roads. The solution times that are presented in this paper naturally depend on many factors. The experiments were executed on a notebook with a mobile Intel i5-4300M CPU and 16GB of RAM memory. In addition to the hardware specifications, the reader may take the following comments under consideration:

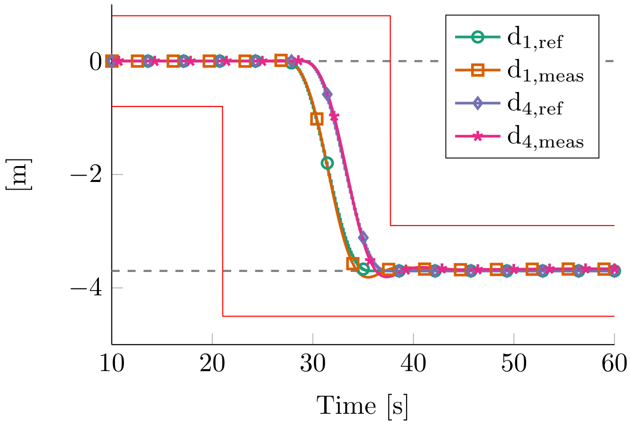

(a) Distance to road geometry with the pre-optimized minimum jerk reference. The lane boundaries are indicated in red.

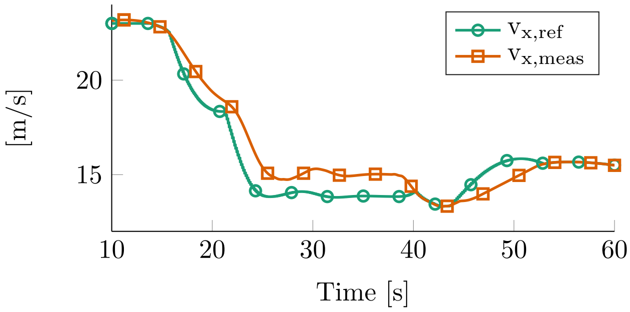

(b) Longitudinal velocity of the tractor and the reference.

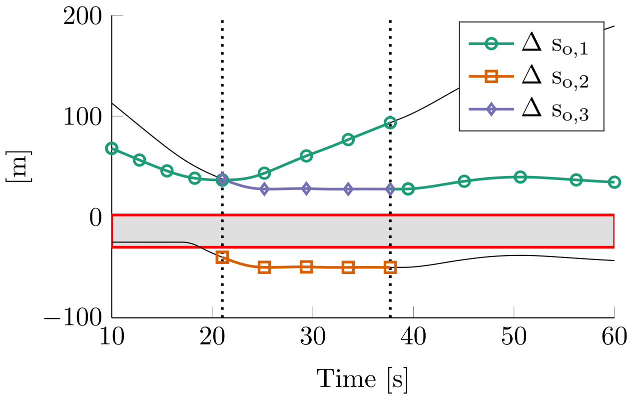

(c) Longitudinal distance to fellow road users with the truck length represented by the gray region. Lane change occurs between dotted lines.

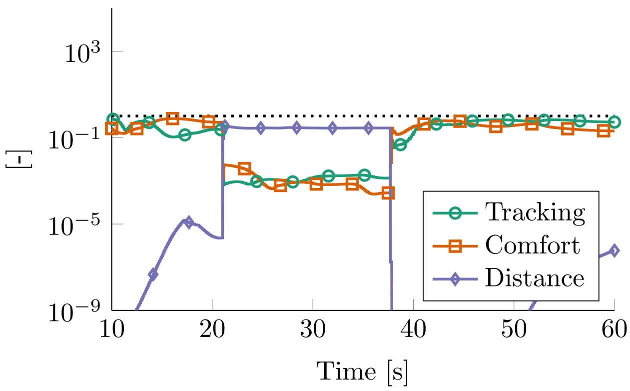

(d) Cost decomposition, normalized with total cost.

Fig. 5. Closed-loop simulation results for ACADO NMPC with high-fidelity plant.

- In the auto-generated RTI scheme from ACADO, the intermediate QPs are condensed and solved with an active-set QP solver. With short horizons this is often the fastest strategy. However, with an increasing horizon, sparsity exploiting QP solvers may become a better alternative. The reader is referred to Frasch et al. (2014) for more details on this issue.
- CasADi provides the option to perform code-generation for the algorithmic differentiation employed for the sensitivity information used in IPOPT. This can naturally speed up computations significantly. This option is not taken into consideration for the presented results.
- In both solution techniques we can parallelize certain elements of the code, e.g., for the multiple-shooting integration step. The computations for results presented in this paper are all serially executed.

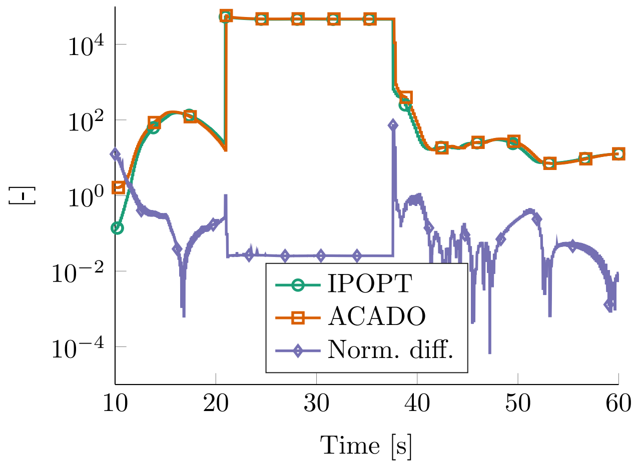

(a) Evolution of the total objective value of both optimization algorithms and the difference normalized with the cost from IPOPT.

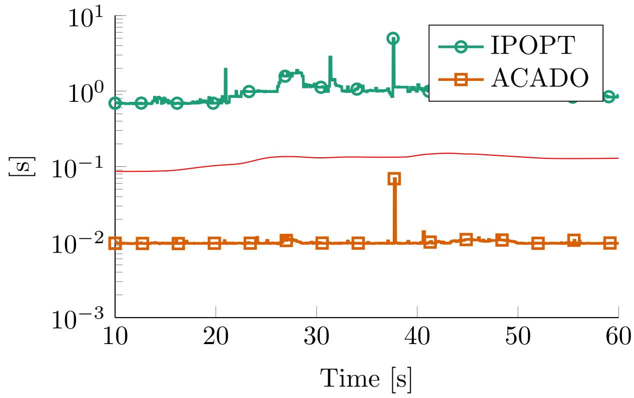

(b) Time consumed by the optimization, with the velocity dependent bound for real-time performance indicated in red.

Fig. 6. Comparison of results for simulations with IPOPT and ACADO.

5. CONCLUSIONS

In this paper we have shown that nonlinear MPC (NMPC) is an appealing method for the trajectory generation of driver assistance systems in long heavy vehicle combinations (LHVCs). All necessary information, such as the geometry of the road and models for the surrounding traffic, can be represented in a natural framework using optimization-based control. From simulation experiment results we observed that real-time performance can be attained for a nonlinear optimization problem. The posed problem was to minimize a cost function that represents a trade-off between driver comfort, reference tracking performance, and distance keeping from surrounding traffic. Simultaneously, constraints on the lateral acceleration, states and controls were enforced. The real-time performance was mainly attributed to the real-time iteration (RTI) scheme and the auto-generated code by the ACADO toolkit. The same problem was also implemented and solved using the interior point NLP-solver IPOPT. We created an interface to IPOPT using the symbolic optimization framework CasADi, employing algorithmic differentiation for all required sensitivity information. We showed that similar closed-loop performance is achieved for the optimal and sub-optimal solution strategies.

The optimal control problem (OCP) in this paper is formulated with a nonlinear least-squares objective. This form is necessary in order to use the generalized Gauss-Newton algorithm in the SQP. Other types of cost functions and solution strategies may be better suited for economic objective functions. Recent work by e.g., Quirynen et al. (2014) present intermediate results to use an exact Hessian in the RTI scheme. These developments are of interest to online nonlinear trajectory generation techniques for LHVCs. The presented control algorithms show that implementation on physical systems is within reach. Future work is aimed at online estimation of the vehicle dynamics, and implementing disturbance estimation to reduce tracking errors due to model mismatch or external disturbances. Additionally, modeling the behavior of surrounding traffic is an open research question that needs to be addressed in more detail. Finally, we ensured a stable closed-loop response by choosing a long enough prediction horizon. We envision guaranteeing recursive feasibility and stability by softening constraints and including a terminal set in the optimization.

The current real-time tractability of NMPC using the RTI iteration scheme enabled us to execute experiments with the presented algorithms in a motion simulator. This served as a basis for a study on driver comfort aimed at introducing truck drivers to future driver assistance systems that has been performed in cooperation between Volvo Group Truck Technology (VGTT) and the Swedish National Road and Transport Research Institute (VTI) in Gothenburg, Sweden.

ACKNOWLEDGEMENTS

Employees of Volvo Group Truck Technology (VGTT) and the Swedish National Road and Transport Research Institute (VTI) are gratefully acknowledged for their assistance that led to the results in this paper.

REFERENCES

ACADO toolkit (2014). ACADO toolkit website. `acadotoolkit.org`.

Andersson, J. (2013). *A General-Purpose Software Framework for Dynamic Optimization*. PhD thesis, Arenberg Doctoral School, KU Leuven.

Borrelli, F., Keviczky, T., and Balas, G.J. (2004). Collision-Free UAV Formation Flight Using Decentralized Optimization and Invariant Sets. In *proceedings of the 43rd IEEE Conference on Decision and Control*, 1099–1104. Nassau, Bahamas.

Diehl, M., Bock, H.G., and Schlöder, J.P. (2005). A Real-Time Iteration Scheme for Nonlinear Optimization in Optimal Feedback Control. *SIAM J. Control Optimization*, 43(5), 1714–1736.

Diehl, M., Findeisen, R., Schwarzkopf, S., Uslu, I., Allgöwer, F., Bock, H.G., Gilles, E.D., and Schlöder, J.P. (2002). An Efficient Algorithm for Optimization in Nonlinear Model Predictive Control of Large-Scale Systems. *Automatisierungstechnik*, 50(12), 557–567.

Ferreau, H.J., Kirches, C., Potschka, A., Bock, H.G., and Diehl, M. (2014). qpOASES: A Parametric Active-Set Algorithm for Quadratic Programming. *Mathematical Programming Computation*, 6(4), 327–363.

Frasch, J.V., Gray, A.J., Zanon, M., Ferreau, H.J., Sager, S., Borrelli, F., and Diehl, M. (2013). An Auto-Generated Nonlinear MPC Algorithm for Real-Time Obstacle Avoidance of Ground Vehicles. In *proceedings of the European Control Conference (ECC13)*, 4136–4141. Zürich, Switzerland.

Frasch, J.V., Vukov, M., Ferreau, H.J., and Diehl, M. (2014). A New Quadratic Programming Strategy for Efficient Sparsity Exploitation in SQP-Based Nonlinear MPC and MHE. In *proceedings of the 18th IFAC World Congress*, 2012, 2945–2950. Milano, Italy.

Gao, Y., Gray, A.J., Frasch, J.V., Lin, T., Tseng, H.E., Hedrick, J.K., and Borrelli, F. (2012). Spatial Predictive Control for Agile Semi-Autonomous Ground Vehicles. In *proceedings of the International Symposium on Advanced Vehicle Control (AVEC12)*. Seoul, South Korea.

Houska, B., Ferreau, H.J., and Diehl, M. (2011). An Auto-Generated Real-Time Iteration Algorithm for Nonlinear MPC in the Microsecond Range. *Automatica*, 47(10), 2279–2285.

Karaman, S. and Frazzoli, E. (2011). Sampling-Based Algorithms for Optimal Motion Planning. *Int. J. Robotics Research*, 30(7), 846–894.

Kindt, M., Burgess, A., Quispel, M., Van Der Meulen, S., and Bus, M. (2011). Monitoring Modal Shift: Longer and Heavier Vehicles, The Follow-Up Measurement. Technical report, Dutch Ministry of Infrastructure and the Environment.

Laine, L. (2007). *Reconfigurable Motion Control Systems for Over-Actuated Road Vehicles*. Ph.D. thesis, Chalmers University of Technology.

LaValle, S.M. (1998). Rapidly-Exploring Random Trees: A New Tool for Path Planning. Technical report, Department of Computer Science, Iowa State University.

Nilsson, P., Laine, L., and Jacobson, B. (2014). Performance Characteristics for Automated Driving of Long Heavy Vehicle Combinations Evaluated in Motion Simulator. In *proceedings of the IEEE Intellicles Vehicles Symposium (IV2014)*, 362–369. Dearborn, USA.

Nilsson, P. and Tagesson, K. (2013). Single-Track Models of an A-Double Heavy Vehicle Combination. Technical report, Chalmers University of Technology, Göteborg, Sweden. URL `http://publications.lib.chalmers.se/records/fulltext/192958/local_192958.pdf`.

Pacejka, H. (2006). *Tyre and Vehicle Dynamics*. Butterworth-Heinemann.

Pivtoraiko, M., Knepper, R.A., and Kelly, A. (2009). Differentially Constrained Mobile Robot Motion Planning in State Lattices. *J. Field Robotics*, 26(3), 308—-333.

Quirynen, R., Houska, B., Vallerio, M., Telen, D., Logist, F., Van Impe, J., and Diehl, M. (2014). Symmetric Algorithmic Differentiation Based Exact Hessian SQP Method and Software for Economic MPC. In *proceedings of the 53rd IEEE Conference on Decision and Control*. Los Angeles, USA.

Rajamani, R. (2012). *Vehice Dynamics and Control*. Springer Science, 2nd edition.

Tagesson, K., Sundström, P., Laine, L., and Dela, N. (2009). Real-time Performance of Control Allocation for Actuator Coordination in Heavy Vehicles. In *proceedings of the IEEE Intellicles Vehicles Symposium (IV2009)*, 685–690.

Van Duijkeren, N. (2014). *Real-Time Receding Horizon Trajectory Generation for Long Heavy Vehicle Combinations on Highways*. Master's thesis, Delft University of Technology. URL `http://resolver.tudelft.nl/uuid:5434052d-b939-4544-92df-ab584b5367d7`.

Verschueren, R., De Bruyne, S., Zanon, M., Frasch, J.V., and Diehl, M. (2014). Towards Time-Optimal Race Car Driving using Nonlinear MPC in Real-Time. In *proceedings of the 53rd IEEE Conference on Decision and Control*, 2505–2510.

Vukov, M., Van Loock, W., Houska, B., Ferreau, H.J., Swevers, J., and Diehl, M. (2012). Experimental Validation of Nonlinear MPC on an Overhead Crane Using Automatic Code Generation. In *proceedings of the American Control Conference (ACC2012)*, 6264–6269. Montréal, Canada.

Wächter, A. and Biegler, L.T. (2006). On the Implementation of Primal-Dual Interior Point Filter Line Search Algorithm for Large-Scale Nonlinear Programming. *Mathematical Programming*, 106(1), 25–57.

Appendix A. CONTROLLER PARAMETERS

The controller tuning parameters employed in the experiments presented in this paper.

Symbol	Value	Symbol	Value
K_{d_1}	800 / 2	K_{d_4}	400 / 2
K_{v_x}	50 / 25	K_{j_x}	50 / 2
K_{j_y}	150 / 3	K_{a_x}	20 / 1.75
$K_{\dot{\delta}}$	1 / 0.05	$K_{\Delta s_{o,k}}$	5000 / 1.2
$\tau_{o,1}$	1.5s	$\tau_{o,2}$	2.5s
$\tau_{o,3}$	1.5s		